Electromagnetic wave sensors

Metal–Dielectric–Metal Metamaterial-Based Hydrogen Sensors in the Water Transmission Window

Sandeep Kumar Chamoli[1,2], Subhash Singh[1,2], and Chunlei Guo[1,2]

[1] *The Guo China–U.S. Photonics Laboratory, State Key Laboratory of Applied Optics, Changchun Institute of Optics, Fine Mechanics and Physics, Chinese Academy of Sciences, Changchun 130033, China*

[2] *University of Chinese Academy of Sciences, Beijing 100039, China*

Manuscript received February 26, 2020; revised March 16, 2020; accepted March 30, 2020. Date of publication April 29, 2020; date of current version May 14, 2020.

Abstract—In this letter, we have numerically proposed design of a novel, efficient, and weather condition independent metal–dielectric–metal metamaterial-based plasmonic hydrogen sensor. In the proposed device, the top and bottom metallic layers are palladium (Pd) nanodisc array and gold thin film, separated by a sandwiched dielectric aluminum oxide layer. The presence of hydrogen reversibly changes Pd to its hydride, which leads to a change in its optical properties. Only 4% (v/v) presence of hydrogen in the air can change optical reflectance from 95% to 14% at 905 nm wavelength, center of first water transmission window, that results for a weather-resistant hydrogen sensor with ∼21.3% change in optical response for 1% change in hydrogen concentration with 76.5 s of response time for remote hydrogen sensing.

Index Terms—Electromagnetic wave sensors, autonomous cars, hydrogen sensor, LIDAR, plasmonic sensing, remote sensing, water transmission window, weather-resistant plasmonic sensor.

I. INTRODUCTION

Recently, research interest in the generation, storage, and sensing of hydrogen is tremendously increased due to its high energy density, clean combustion, and applications in the production of commodity chemicals [1], [2]. Owing to low ignition energy of 0.02 mJ and high heat combustion of 285.8 kJ/mol, hydrogen possesses explosive nature with high flammability. Hydrogen storage has always been challenging owing to its minimum 4% explosion limit; therefore, careful observation of hydrogen level is highly required in activities related to its practice to forbid explosions. Due to its odorless and colorless properties, it is challenging to detect a low concentration of hydrogen without an appropriate sensor. This problem leads to the design of a hydrogen sensor that can detect the leakage of a low concentration of hydrogen for its safe use, storage, and transportation to prevent explosion [3].

Several hydrogen sensors are reported to date for the early detection of hydrogen leakage using different materials and principles [4]–[7]. Most of the sensors previously reported are electrical, not optical, that needs the presence of a complete sensor unit in the test area. Surface plasmon resonance (SPR) properties of materials are widely used to increase the efficiency of photonics and optoelectronic devices [8], waveguides [9], enhanced transmission [10], and plasmonic sensors [11]. Optical or plasmonic sensors have several advantages over their electrical analog including remote sensing, intrinsically safe and multiplexing possibilities [12], [13]. Due to its remote detection capabilities, optical hydrogen sensors are more sensitive and reliable, if conditions between source and detector are stable. However, changes in the weather conditions such as rain, fog, snow, and increased humidity severely attenuate the light signal, before and after its interaction from the plasmonic system, resulting in a dramatic degradation in its performance and reliability. To conquer the weather challenge, it is desirable to design a weather-proof plasmonic sensor operating in one of the water transmission windows centered at 905 and 1550 nm wavelengths. In most of the previous reports [14]–[16], researchers designed, fabricated and tested plasmonic hydrogen sensors under laboratory conditions, and completely ignored challenges that could be faced in the practical implementation of these sensors in the field conditions. Water poses a ten times larger extinction coefficient at 1550 nm as compared to 905 nm that allows 905 nm systems more weather-proof over 1550 nm [17]. Therefore, optical sensors that will operate at 905 nm will be less prone to rain, fog, snow, and ambient humidity as compared to those operating at 1550 nm.

To the best of our knowledge, this letter is the first report on the theoretical design and numerical demonstration of a fast plasmonic metal–dielectric–metal (MDM) metamaterial-based hydrogen sensor operating at 905 nm wavelength. The geometric parameters of the MDM plasmonic system such as radius of palladium (Pd) nanodiscs, its period, and thickness of the dielectric layer are optimized to get high optical absorption near 900 nm. The presence of hydrogen reversibly changes Pd to its hydride, which leads to a change in its optical properties and reflectance of the incident light signal. Only 0% to 4% (v/v) change in the hydrogen concentration in the air can change optical reflectance from 95% to 14% at 905 nm wavelength that results in a weather-resistant hydrogen sensor with 20.25 sensitivity and 76.5 s of response time for remote hydrogen sensing.

II. DESIGN AND SIMULATION PARAMETERS

Fig. 1 shows the proposed MDM metamaterial plasmonic structure. The top and bottom layers are a 2-D array of Pd nanodisc and plasmonic active metal, respectively, separated by a thin aluminum oxide (Al_2O_3) spacer layer as a dielectric medium. The length and breadth of metallic and dielectric rectangular layers are the same as a, the thickness of

Corresponding authors: Subhash Singh; Chunlei Guo (ssingh49@ur.rochester.edu; guo@optics.rochester.edu).

Associate Editor: X. Shu.
Digital Object Identifier 10.1109/LSENS.2020.2991081

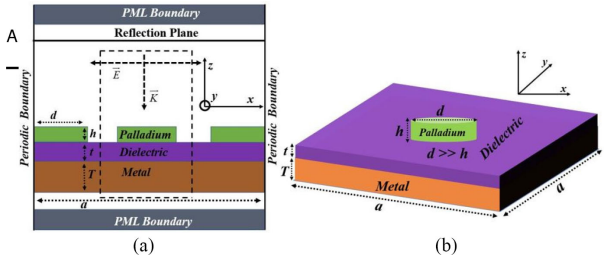

Fig. 1. (a) Two-dimensional view of the proposed MDM metamaterial structure. The dashed lines represent a unit cell of the periodic structure, enclosing the grating in the middle. The incident wave is traveling $\vec{K}$ in the negative *y*-direction. Electric field $\vec{E}$ oscillations are in the *x*-direction. (b) Geometric diagram of a one-unit cell of the proposed hydrogen sensor, *a* is the side of the rectangular metallic and dielectric film with *t* and *T* are the thickness, and *h* and *d* are diameter and height of Pd grating on the top.

dielectric and the metal film are t and T, respectively, whereas d and h are the diameter and height of Pd nanodisc grating.

A finite-difference time-domain method developed by Yee was used to simulate the optical response of the designed plasmonic system using commercial software from Lumerical Solution Inc. [19].

Lorentz–Drude's material model was used to calculate the optical constants of metals [18]. Perfectly matched layer (PML) boundary conditions are used in the *Z*-direction, whereas periodic boundary conditions are used in the *X*- and *Y*-direction. A 3-D simulation has been used to estimate the optical response in the grating structure. The light is incident normally, which is propagating in the *Z*-direction and polarized in the *X*-direction. To achieve optical reflection data, an optical power monitor is placed in between the source and upper PML boundary. Generally, a shift in the resonance wavelength of an SPR-based refractive index sensor is due to the change in the refractive index of the surrounding medium [19]. Air is considered as a surrounding medium for hydrogen sensors and with an increase in the hydrogen concentration from 0% to 4% there is not a significant change in the ambient refractive index. Therefore, conventional metallic systems are not suitable for hydrogen sensing applications. As 4% hydrogen concentration in the air is the limit for an explosion, therefore sensing of smaller volume of hydrogen in the air is required. According to the literature, Pd is the best choice for hydrogen detection, where Pd reversibly forms PdH_x [20] in the presence of hydrogen (x represents the atomic ratio of H/Pd) following:

$$\mathrm{Pd} + \frac{x}{2}\mathrm{H_2} \leftrightarrow \mathrm{PdH}_x. \tag{1}$$

Absorption of hydrogen in the Pd lattice increases its volume, and therefore, a decrease in free-electron density that results in a change in its permittivity. The shift in the resonance wavelength can be understood with the complex permittivity of Pd using the following equation [21]:

$$\varepsilon_{\mathrm{Pd,c\%H_2}} = h(c) \times \varepsilon_{\mathrm{Pd,0\%H_2}} \tag{2}$$

where $\varepsilon_{\mathrm{Pd,0\%H_2}}$ and $\varepsilon_{\mathrm{Pd,c\%H_2}}$ are the complex permittivity of Pd in the presence and absence of hydrogen gas, and $h(c)$ is a nonlinear parameter that decreases with increasing hydrogen concentration c %. The values of $h(c)$ are 1.0 and 0.8 for 0% and 4% (v/v) hydrogen concentrations, respectively [21].

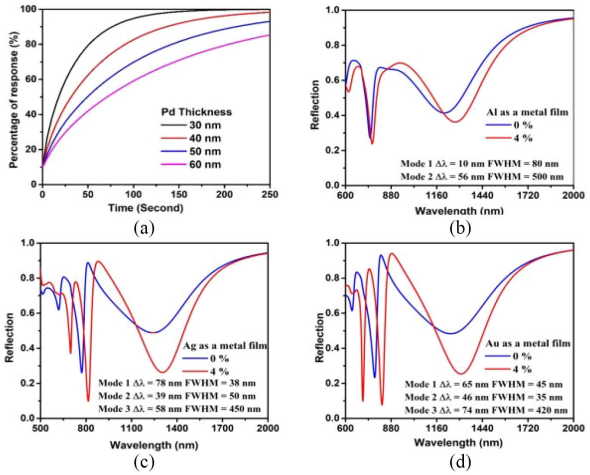

Fig. 2. (a) Percentage of response as a function of Pd thickness and reflection response for 0% and 4% hydrogen concentration for (b) Al, (c) Ag, and (d) Au.

III. RESULT AND DISCUSSIONS

A. Time Analysis and Reflection Response

The response time of a sensor to detect hydrogen leakage is equally important to analyze. We followed the theoretical analysis of the reaction between hydrogen and Pd to understand the response time of the proposed structure following Liu *et al.* [22]. The percentage of response η exponentially depends on the response time (T_{response}) as follows:

$$\eta \approx 1 - \frac{8}{\pi^2}\exp\left(-D\frac{\pi^2 T_{\mathrm{response}}}{4h^2}\right) - \frac{8}{9\pi^2}\exp\left(-D\frac{9\pi^2 T_{\mathrm{response}}}{4h^2}\right) = 90\%. \tag{3}$$

In (3), normally the value of T_{response} switches from several seconds to 10 min. The stability in hydrogen reading can be seen as T_{response} tends to infinity with percentage response reaching to 100. Practically response value of 90% is considered as a stable measurement. Time taken from the initial reaction to reach 90% of stability is known as response time (T_{response}). Therefore, it is required for T_{response} to satisfy (3). The second term of (3) is negligible as compared to the first term that simplifies (3) as follows:

$$1 - \frac{8}{\pi^2}\exp\left(-D\frac{\pi^2 T_{\mathrm{response}}}{4h^2}\right) = 90\%. \tag{4}$$

Thus, we can say that the response time of the hydrogen sensor depends on the thickness (h) of Pd discs, and diffusion coefficient (D) of hydrogen in Pd lattice. Therefore, a decrease in the Pd thickness and an increase in its diffusion coefficient can definitely reduce the response time to detect the leakage of hydrogen as early as possible. Assuming the diffusion coefficient 10 $\mathrm{nm^2/s}$, as taken from [21]

$$T_{\mathrm{response}} = \frac{4h^2}{D\pi^2}\ln\frac{\pi^2}{80} \approx 0.85\frac{h^2}{D}. \tag{5}$$

The percentage response as a function of Pd thickness and response time for the proposed sensor is calculated and demonstrated in Fig. 2(a). It is clear from Fig. 2(a) that in order to achieve a 100% response for 30-nm-thick Pd disk, a time of 150 s is required. Response percentage is increasing with decreasing Pd thickness from 30 to

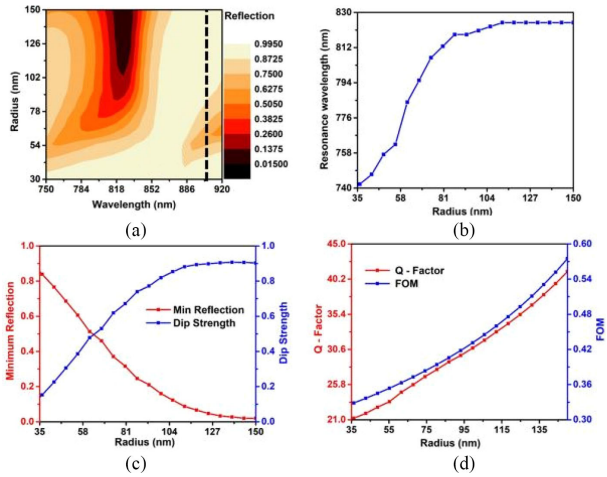

Fig. 3. (a) Reflection as a function of Pd nanodisk radius and wavelength. (b) Resonance wavelength corresponds Pd nanodisk radius. (c) Minimum reflection and dip strength as a function of Pd nanodisk radius. (d) Q-factor and FOM as a function of Pd nano.

60 nm. The response time of the proposed sensor for 30-nm-thick Pd nanodisc is calculated to be 76.5 s following (5), which is the lowest response time for the hydrogen sensor. Similarly, the calculated recovery time ($T_{rec.}$), time to change response from 90% to 10%, for the same device is 106 s. In order to understand the hydrogen sensing ability of the proposed MDM metamaterial structure, first, we have investigated the spectral reflection response of the plasmonic system for three SPR active metals such as Al, Silver (Ag) and gold (Au). Fig. 2(b)–(d) demonstrates the SPR response for Al, Ag, and Au, respectively, for 0 and 4% (v/v) hydrogen concentration. The shift in the resonance wavelength can be understood from (2), which states that on increasing hydrogen concentration the complex permittivity of Pd decreases resulting shift in the resonance wavelength. The values of full-width at half-maximum (FWHM) and shift in the resonance wavelength ($\Delta\lambda$) corresponding to Al, Ag, and Au plasmonic metals as bottom layer can be seen in the corresponding insets. Having a minimum FWHM, a maximum shift in the resonance wavelength ($\Delta\lambda$), maximum dip strength, and a minimum reflection for 0 and 4% hydrogen concentrations, we choose Au as a metallic layer in the proposed plasmonic system. The second mode of the Au plasmonic system [see Fig. 2(d)] is exploited further for sensing analysis.

B. Optimized Figure of Merit (FOM) for the Proposed Hydrogen Sensor

Sensitivity of the plasmonic system can be defined as follows [23]: $S = \Delta\lambda_{res}/\Delta C_{H_2}$, where λ_{res} and C_{H_2} are the shift in resonance wavelength and hydrogen concentration. FOM, for better evaluation of geometrical and simulation parameters, can be expressed as follows: FOM $= SQ/\lambda_{res}$, where Q is the quality factor given by $Q = \lambda_{res}/\text{FWHM}$, where λ_{res} is the resonance wavelength.

In the following sections, we will present the optimization of geometric parameters (radius (r), grating period (Λ), and spacer thickness (t)) of the proposed MDM metamaterial for 4% hydrogen concentration. In all three cases, optimization has been done by calculating FOM and quality Q-factor. A normally incident broadband light in the wavelength range of 600–900 nm is considered a light source. The contour plot for the reflection spectrum as a function of Pd nanodisc radius and wavelength is shown in Fig. 3(a). A clear redshift in the resonance wavelength can be seen on increasing the radius of nanodisk [see Fig. 3(b)]. This is due to increased coupling between conduction

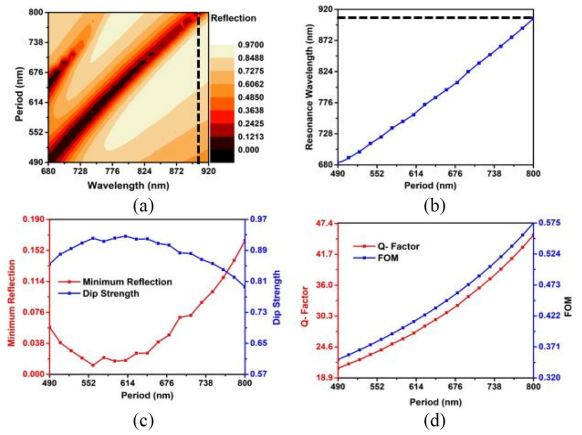

Fig. 4. (a) Reflection as a function of grating period and wavelength. (b) Resonance wavelength corresponds grating period. (c) Minimum reflection. (d) Q-factor and FOM as a function of grating period.

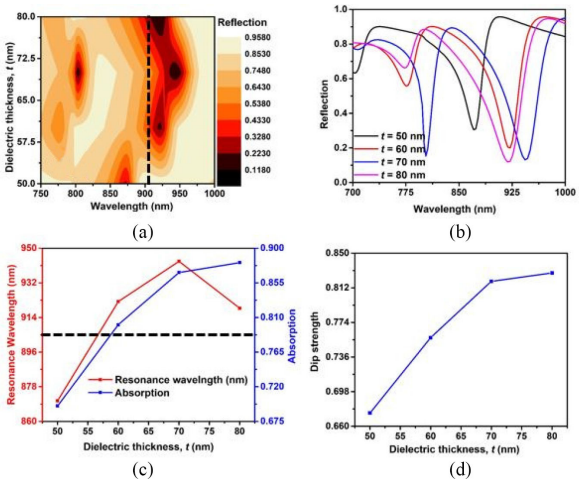

Fig. 5. (a) Contour plot for reflection as a function of dielectric thickness and wavelength. (b) Reflection as a function of dielectric spacer. (c) Dielectric thickness versus resonance wavelength and absorption (right). (d) Dip strength with dielectric.

electrons and incident light photons. For this simulation, we kept the height and grating period fixed at 30 and 700 nm, respectively. The Q-factor, dip strength, FOM, and minimum reflection are extracted from the spectral reflectance response of plasmonic systems with different radius of Pd discs [see Fig. 3(c) and (d)]. So, we can conclude that 105–150 nm can be considered as an appropriate choice for Pd nanodisc radius.

In order to choose a proper grating period, we have optimized the grating period of the proposed MDM metamaterial structure. Fig. 4(a) represents the reflection contour plot as a function of grating period and wavelength. The resonance wavelength and the grating period follow the linear relationship as shown in Fig. 4(b). On increasing the grating period corresponding changes in minimum reflection value, dip strength, Q-factor, and FOM are calculated and outlined in Fig. 4(c) and (d).

From Figs. 3 and 4, we can conclude that maximum FOM of 0.52 corresponds to disc radius of 150 nm and a period of 800 nm to get SPR absorption close to 905 nm. The FOM and Q-factor can be improved by reducing the FWHM of reflection spectra through varying the thickness and refractive index of dielectric layer. Fig. 5 demonstrates the effect of dielectric thickness sandwiched between Pd nanodisc and Au film and

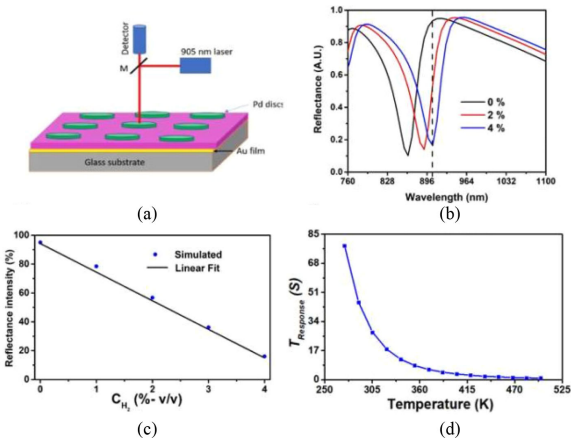

Fig. 6. (a) Schematic design of the proposed device with arrangement of a light source and a detector. (b) Reflectance response of the optimized ($r = 150$ nm, $\Lambda = 800$ nm, $h = 30$ nm, and $t = 50$ nm) structure with broadband illumination for 0% and 4% (v/v) of hydrogen concentration. (c) % reflectance at 905 nm with hydrogen concentration in the air. (d) Variation in the response time of the proposed hydrogen sensor with temperature.

can be understood by the equivalent *RLC* model as explained in this work [24]. The top Pd nanodisc and bottom Au film grant coupling of the magnetic field due to the presence of antiparallel current between two metallic films. Therefore, through increasing the thickness of the dielectric layer, the magnetic field response can be tuned. Fig. 5(a) and (b) illustrates the reflection response with varying thickness of the dielectric spacer. Further, we can see the resonance wavelength, absorption, and dip strength for different thickness of the dielectric spacer layer from Fig. 5(c) and (d). The SPR position of second resonance mode shows a longer wavelength shift with enhancement in the dip strength with an increase in the spacer layer thickness.

Fig. 6(a) shows the schematic of our proposed hydrogen sensing device, where a 905-nm laser beam normally illuminates the plasmonic system and reflected to the detector. From previous optimizations, we chose $r = 150$ nm, $\Lambda = 800$ nm, $h = 30$ nm, and $t = 50$ nm geometric parameters for plasmonic structure. An increase in the percentage hydrogen concentration (v/v) causes longer wavelength shifts in the SPR peak position [see Fig. 6(b)]. Reflectance values at 905 nm wavelength for different hydrogen concentrations is linearly fitted [see Fig. 6(c)] to get sensitivity ($S = \frac{\Delta R/R_0}{\Delta C_H}$, where ΔC_H is change in hydrogen concentration) of 20.25 for the proposed hydrogen sensor. The diffusion coefficient of an active material increases with increasing temperature (T) following the Arrhenius law $D = D_0 \exp(-E/K_B T)$, where D_0, E, and K_B are diffusing coefficient at 0 K, activation energy of the material used, and Boltzmann constant, respectively, resulting in a decrease in the response time of the proposed hydrogen sensor (5) with increase in the temperature [see Fig. 6(d)].

IV. CONCLUSION

We proposed the design of a novel, efficient, and weather condition independent MDM metamaterial-based plasmonic hydrogen sensor. In the proposed device, the top and bottom metallic layers are Pd nanodisc array and Au thin film, separated by a sandwiched dielectric (Al_2O_3) layer. The presence of hydrogen reversibly changes Pd to its hydride, which leads to a change in its optical properties. Only 4% (v/v) presence of hydrogen in the air can change optical reflectance from 95% to 12% at 905 nm wavelength, i.e., the center of first water transmission window, that results for a weather-resistant hydrogen sensor with ~22% change in optical response for 1% change in hydrogen concentration with 76.5 s of response time for remote hydrogen sensing. Present research can open the door for remote monitoring of hydrogen production, hydrogen storage, and hydrogen filling stations to popularize hydrogen-powered vehicles.

ACKNOWLEDGMENT

This work was supported in part by the National Key R&D Program of China under Grant 2017YFB1104700, in part by the National Natural Science Foundation of China under Grant 11674178, and in part by the Jilin Provincial Science and Technology Development Project under Grant 20180414019GH. The work of S. K. Chamoli was supported by "CAS-TWAS Presidential's Fellowship for International Doctorate Students."

REFERENCES

[1] B. Lai *et al.*, "Hydrogen evolution reaction from bare and surface functionalized few layered MoS_2 in alkaline electrolytes," *Mater. Today Chem.*, vol. 14, 2019, Art. no. 100207.
[2] W. Yu *et al.*, "Ag2S quantum dots as an infrared excited photocatalyst for hydrogen production," *ACS Appl. Energy Mater.*, vol. 2, no. 4, pp. 2751–2759, 2019.
[3] S. H. N. Yousef and S. Mashareh, "Hydrogen leakage sensing and control: (Review)," *Biomed. J. Sci. Tech. Res.*, vol. 21, no. 5, pp. 16228–16240, 2019.
[4] J. D. Fowler, S. Virji, R. B. Kaner, and B. H. Weiller, "Hydrogen detection by polyaniline nanofibers on gold and platinum electrodes," *J. Phys. Chem. C*, vol. 113, no. 16, pp. 6444–6449, 2009.
[5] S. Krishnan, R. Joshi, P. K. Sekhar, and S. Bhansali, "Nanocrystalline palladium thin films for hydrogen sensor application," *Sensor Lett.*, vol. 7, no. 1, pp. 31–37, 2009.
[6] K. Skucha, Z. Fan, K. Jeon, A. Javey, and B. Boser, "Palladium/silicon nanowire Schottky barrier-based hydrogen sensors," *Sensors Actuators B, Chem.*, vol. 145, no. 1, pp. 232–238, 2010.
[7] Q. Huang, D. Zeng, H. Li, and C. Xie, "Room temperature formaldehyde sensors with enhanced performance, fast response and recovery based on zinc oxide quantum dots/graphene nanocomposites," *Nanoscale*, vol. 4, pp. 5651–5658, 2012.
[8] B. Wang, S. C. Singh, H. Lu, and C. Guo, "Design of aluminum bowtie nanoantenna array with geometrical control to tune LSPR from UV to near-IR for optical sensing," *Plasmonics*, 2019, doi: 10.1007/s11468-019-01071-z.
[9] Y. Chaonan, S. C. Singh, M. ElKabbash, J. Zhang, H. Lu, and C. Guo, "Quasi-rhombus metasurfaces as multimode interference couplers for controlling the propagation of modes in dielectric-loaded waveguides," *Opt. Lett.*, vol. 44, no. 7, pp. 1654–1657, 2019.
[10] J. Zhang *et al.*, "Plasmonic metasurfaces with 42.3% transmission efficiency in the visible," *Light, Sci. Appl.*, vol. 8, no 1, pp. 53–65, 2019.
[11] S. K. Chamoli, S. C. Singh, and C. Guo, "Design of extremely sensitive refractive index sensors in infrared for blood glucose detection," *IEEE Sensor J.*, vol. 20, no. 9, pp. 4628–4634, May 2020.
[12] Z. Yang *et al.*, "Extrinsic Fabry-Perot interferometric optical fiber hydrogen detection system," *Appl. Opt.*, vol. 49, no. 15, pp. 2736–2740, 2010.
[13] M. Aleixandre *et al.*, "Optic fiber used as sensor to measure low hydrogen concentrations," *Proc. SPIE*, vol. 6593, 2007, Art. no. 65930Y.
[14] M. Eryurek *et al.*, "Optical sensor for hydrogen gas based on a palladium-coated polymer microresonator," *Sensors Actuators B, Chem.*, vol. 212, pp. 78–83, 2015.
[15] N. A. Yebo *et al.*, "Silicon-on-insulator (SOI) ring resonatorbased integrated optical hydrogen sensor," *IEEE Photon. Technol. Lett.*, vol. 21, no. 14, pp. 960–962, Jul. 2009.
[16] B. D. Adams and A. Chen, "The role of palladium in a hydrogen economy," *Mater. Today*, vol. 14, no. 6, pp. 282–289, 2011.
[17] J. Wojtanowski, M. Zygmunt, M. Kaszczuk, and Z. Mierczyk, "Comparison of 905 nm and 1550 nm semiconductor laser rangefinders' performance deterioration due to adverse environmental conditions," *Opto-Electron. Rev.*, vol. 22, no. 3, pp. 183–190, 2014, doi: 10.2478/s11772-014-0190-2.
[18] L. Inc. Lumerical Solutions, Inc. Retrieved https://www.lumerical.com/products/fdtd-solutions/.s
[19] E. D. Palik, *Handbook of Optical Constants of Solids II*, vol. 1. Boston, MA, USA: Academic, 1991, pp. 77–135.
[20] X. Bevenot *et al.*, "Surface plasmon resonance hydrogen sensor using an optical fibre," *Meas. Sci. Technol.*, vol. 13, pp. 118–124, 2002.
[21] P. Tobiška *et al.*, "An integrated optic hydrogen sensor based on SPR on palladium," *Sensors Actuators B, Chem.*, vol. 74, no. 1–3, pp. 168–172, 2001.
[22] Y. Liu *et al.*, "Modeling of hydrogen atom diffusion and response behavior of hydrogen sensors in Pd-Y alloy nanofilm," *Sci. Rep.*, vol. 6, 2016, Art. no. 37043.
[23] K. Cicek *et al.*, "Single-slot hybrid microring resonator hydrogen sensor," *J. Opt. Soc. Amer. B*, vol. 34, pp. 1465–1470, 2017.
[24] T. Sellier *et al.*, "Resonant circuit model for efficient metamaterial absorber," *Opt. Express* vol. 21, no. S6, pp. A997–A1006, 2013.